



**UvA-DARE (Digital Academic Repository)**

**Real-time x-ray diffraction study of concentration profiles in CuCl<sub>2</sub>-intercalated graphite during deintercalation**

Capkova, P.; Rafaja, D.; Walter, R.; Boehm, H.P.; van Malssen, K.F.; Schenk, H.

*Published in:*  
Carbon

*DOI:*  
[10.1016/0008-6223\(95\)00091-Q](https://doi.org/10.1016/0008-6223(95)00091-Q)

[Link to publication](#)

*Citation for published version (APA):*

Capkova, P., Rafaja, D., Walter, R., Boehm, H. P., van Malssen, K. F., & Schenk, H. (1995). Real-time x-ray diffraction study of concentration profiles in CuCl<sub>2</sub>-intercalated graphite during deintercalation. *Carbon*, 33, 1425-1432. DOI: 10.1016/0008-6223(95)00091-Q

**General rights**

It is not permitted to download or to forward/distribute the text or part of it without the consent of the author(s) and/or copyright holder(s), other than for strictly personal, individual use, unless the work is under an open content license (like Creative Commons).

**Disclaimer/Complaints regulations**

If you believe that digital publication of certain material infringes any of your rights or (privacy) interests, please let the Library know, stating your reasons. In case of a legitimate complaint, the Library will make the material inaccessible and/or remove it from the website. Please Ask the Library: <http://uba.uva.nl/en/contact>, or a letter to: Library of the University of Amsterdam, Secretariat, Singel 425, 1012 WP Amsterdam, The Netherlands. You will be contacted as soon as possible.



0008-6223(95)00091-7

REAL-TIME X-RAY DIFFRACTION STUDY OF  
CONCENTRATION PROFILES IN  $\text{CuCl}_2$ -INTERCALATED  
GRAPHITE DURING DEINTERCALATIONP. ČAPKOVÁ,<sup>1</sup> D. RAFAJA,<sup>1</sup> J. WALTER,\*<sup>2</sup> H. P. BOEHM,<sup>2</sup> K. F. van MALSSSEN,<sup>3</sup>  
and H. Schenk<sup>3</sup>.<sup>1</sup>Faculty of Mathematics and Physics, Charles University Prague, Ke Karlovu 5, 12116 Prague,  
Czech Republic<sup>2</sup>Institut für Anorganische Chemie, Ludwig Maximilians Universität, Meisestr. 1, 80333 Munich, Germany<sup>3</sup>Laboratory for Crystallography, University of Amsterdam, Nieuwe Achtergracht 166,  
1018 WV Amsterdam, The Netherlands

(Received 21 March 1995; accepted in revised form 10 May 1995)

**Abstract**—Deintercalation of  $\text{CuCl}_2$ -intercalated graphite has been studied under two different conditions: during exposure to ambient air and to boiling water. The real-time X-ray powder diffraction method was used to follow the diffusion-controlled deintercalation reaction. The estimation of the phase composition at any time during the reaction enabled us to visualize the development of concentration profiles in the disk-shaped particles of intercalate during the deintercalation. The detailed analysis of the diffraction line profiles the line positions revealed differences and also common features of the concentration gradients established by decomposition in ambient air and in boiling water. Conclusions concerning the mechanism of deintercalation and staging phase transitions based on the present experimental results are compared with the theoretical predictions.

**Key Words**—Graphite intercalation compounds, deintercalation, staging, concentration gradient, real-time XRD method.

## 1. INTRODUCTION

The poor stability of the graphite intercalation compounds (GIC) is the crucial factor in the practical applications of these materials. Although theoretical studies have been presented dealing with the mechanism and kinetics of intercalation and staging phase transition, (see e.g. Kirczenow[1], Safran[2], Anderson Axdal and Chung[3]), there is a lack of experimental evidence for their conclusions, concerning the phase diagram structure, staging mechanism, staging transitions and stage disorder. The results of the existing theoretical studies lead to the conclusions summarized below.

The staging mechanism in GIC is described as a balance of two main interactions: the interaction between the intercalant and host layers and the electrostatic repulsions of the intercalant layers due to a charge transfer between the intercalant and host layers[1]. According to Safran and Hamann[4], not only electrostatic effects but also long-range elastic interactions are responsible for staging.

On the basis of the calculated equilibrium phase diagrams, Kirczenow[1] suggested the staging transitions to be continuous, proceeding via stage-disordered states; that means that during intercalation the crystal passes through all stages  $n > n_0$ , before reaching the final equilibrium stage  $n_0$ . The regions of pure stages  $n$  and  $n - 1$  are separated by a

band of mixed disordered stage, where the sequence of layers is an irregular binary mixture of  $c$ -parameters corresponding to stages  $n$  and  $n - 1$ . These interfaces between the pure stages migrate through the sample during intercalation (resp. deintercalation). According to Kirczenow[1], the extreme sharpness of stage transitions in the case of low stages makes it difficult to distinguish experimentally between first-order and continuous transitions, and the very narrow interfaces between pure stages are difficult to detect. The Daumas-Hérol domain model[5] is widely accepted as the only reasonable explanation for the intercalation process and staging transitions. The phase transitions, in which the stage index  $n$  changes, can occur through the movement of microscopic islands of intercalant atoms.

As to the stage disorder, Kirczenow[1] has shown that:

- The stage disorder is very sensitive to the interlayer repulsion (charge transfer between host and guest atoms).
- The stage disorder regions increase with increasing temperature.
- The stage disorder regions increase with increasing stage index.
- Stage disorder is less for the larger domain sizes.
- The stage disorder should not be influenced significantly by in-plane order of the intercalants or lack of in-plane order or whether the intercalant layers are commensurate or incommensurate to the host lattice.

\*Present address: Naturhistorisches Museum, Burggring 7, A-1014 Vienna, Austria.

In this paper we present the results of real-time X-ray diffraction study of the deintercalation reaction in powder samples of  $\text{CuCl}_2$ -intercalated graphite during decomposition in ambient air and in boiling water. The temperature and humidity are crucial factors affecting the structural stability and are important as to the possible practical applications (see e.g. Ansart[6]). In the present work, we used boiling water to combine both effects and to speed up the deintercalation reaction. We followed the changes in the diffraction pattern by use of a position sensitive detector. The detailed analysis of diffraction line profiles and line positions enabled us to determine the phase composition and consequently to estimate the concentration gradient in powder particles at any time of reaction. This result is especially interesting for the possible practical applications of  $\text{CuCl}_2$ -intercalated graphite. Conclusions concerning the mechanism of deintercalation and staging transitions based on the present results confirm most of the theoretical predictions summarized above.

## 2. EXPERIMENTAL CONDITIONS AND DATA ANALYSIS

The real-time X-ray powder diffractometer was constructed in the Laboratory for Crystallography, University of Amsterdam. A non-conventional diffraction geometry with the flat powder sample in a horizontal position, is used in the present measurements, and has been described in detail by van Malssen, Peschar and Schenk[7]. The  $2-\theta$  range recorded with the flat position-sensitive detector EG&G 1472 (1024 diodes) was  $17.65-32.15^\circ$ .  $\text{Cu}_{K\alpha 1}$  radiation ( $\lambda=1.5405 \text{ \AA}$ ) was used, with a graphite monochromator in primary beam.

The  $\text{CuCl}_2$ -intercalated graphite has been prepared in the Institute for Inorganic Chemistry, University of Munich. A transport reaction via the gas phase was used for the intercalation of  $\text{CuCl}_2$  into natural graphite from Kropfmühl (Bavaria). The diameter of graphite flakes was about 0.2–1 mm, with an average estimated to be 0.32 mm. The graphite and anhydrous copper(II)-chloride were mixed in an ampoule. This mixture contained a small excess of copper chloride with respect to the reported stoichiometric composition for stage 2[8]. The tube was evacuated and a small amount of chlorine gas was condensed in it. The tube was then sealed and heated for 4 days at  $400^\circ\text{C}$ .

The measurements during decomposition in open air were started 10 minutes after the opening of the glass ampoule with the  $\text{CuCl}_2$ -intercalated graphite (this time was necessary for the sample preparation); 25 measurements of the diffraction diagram were carried out under the following conditions: measuring time 120 seconds; pause between measurements 8 minutes; air humidity 65%, and air temperature  $22^\circ\text{C}$ .

In case of deintercalation in boiling water, the powder sample was placed into a glass dish with boiling water, and after the exposure the powder was taken out quickly, slightly pressed into the sample

holder, and measured (120 seconds). For every new measurement, the powder sample had to be pressed into a new sample holder, and this could easily cause a slight displacement of sample surface with respect to the goniometer axis. To correct for such misalignment, the intercalate was mixed with corundum powder as a standard, used for the rescaling of all the data files.

Data treatment is based on the complex profile analysis of the diffraction pattern, including the peak maxima, integrated intensities and profile asymmetry determination. The unraveling of the diffraction profile into separate components, corresponding to the individual phases (stages), was performed by use of the DIFPATAN program[9]. The asymmetric Pearson function has been used to fit the measured diffraction profiles. Quantitative phase analysis during the deintercalation reaction has been performed using the Chung method[10]. The 001 structure factors and unit cell volumes were included into the calculation of the volume fraction of the individual components. The approximation suggested by Vila and Ruiz-Amil[11] was used for the calculation of structure factors for mixed stages.

## 3. EVOLUTION OF THE DIFFRACTION PATTERN IN AMBIENT AIR AND BOILING WATER

The evolution of the diffraction pattern is illustrated in Figs 1 and 2 for 10 and 60 minutes, respectively, in ambient air and in Figs 3 and 4 for 5 and 60 minutes, respectively, in boiling water. As usual, in the case of the layered structures, only 001 reflections have been observed in the diffraction patterns. The full measured  $2-\theta$  range was split into two parts for the profile fitting. The first part (a) within  $2-\theta$   $18.8-24.3^\circ\text{C}$  contains the lines 002 stage 1, 003 stage 2, 004 stage 3, 005 stage 4 and 006 stage 5. This first part is more convenient for the phase analysis of low index stages because of the strong overlap of peaks in the second part (b) within the  $2-\theta$  range  $24.6-29.1^\circ\text{C}$ .

Nevertheless, this overlapping part must be used for the estimation of graphite and higher stages content. The presence of the higher stage packages manifests itself by increasing peak between the positions for stage 5 and graphite. (See the second parts of Figs 1–4.)

The peak positions for the pure stages marked by vertical lines were calculated from  $c_1 = 9.40 \text{ \AA}$  [10] for stage 1 of  $\text{CuCl}_2$ -intercalated graphite using the formula

$$c_n = (n-1)c_0 + c_1 \quad (1)$$

where  $n$  is the stage index,  $c_1$  is the spacing of stage 1, and  $c_0 = 3.35 \text{ \AA}$  is the distance between adjacent carbon planes. The distances  $c_0$  and  $c_1$  are assumed to be stage independent. The analysis of the one-dimensional Patterson function in the  $c$ -direction [12] confirmed the published values for  $\text{CuCl}_2$ -graphite.

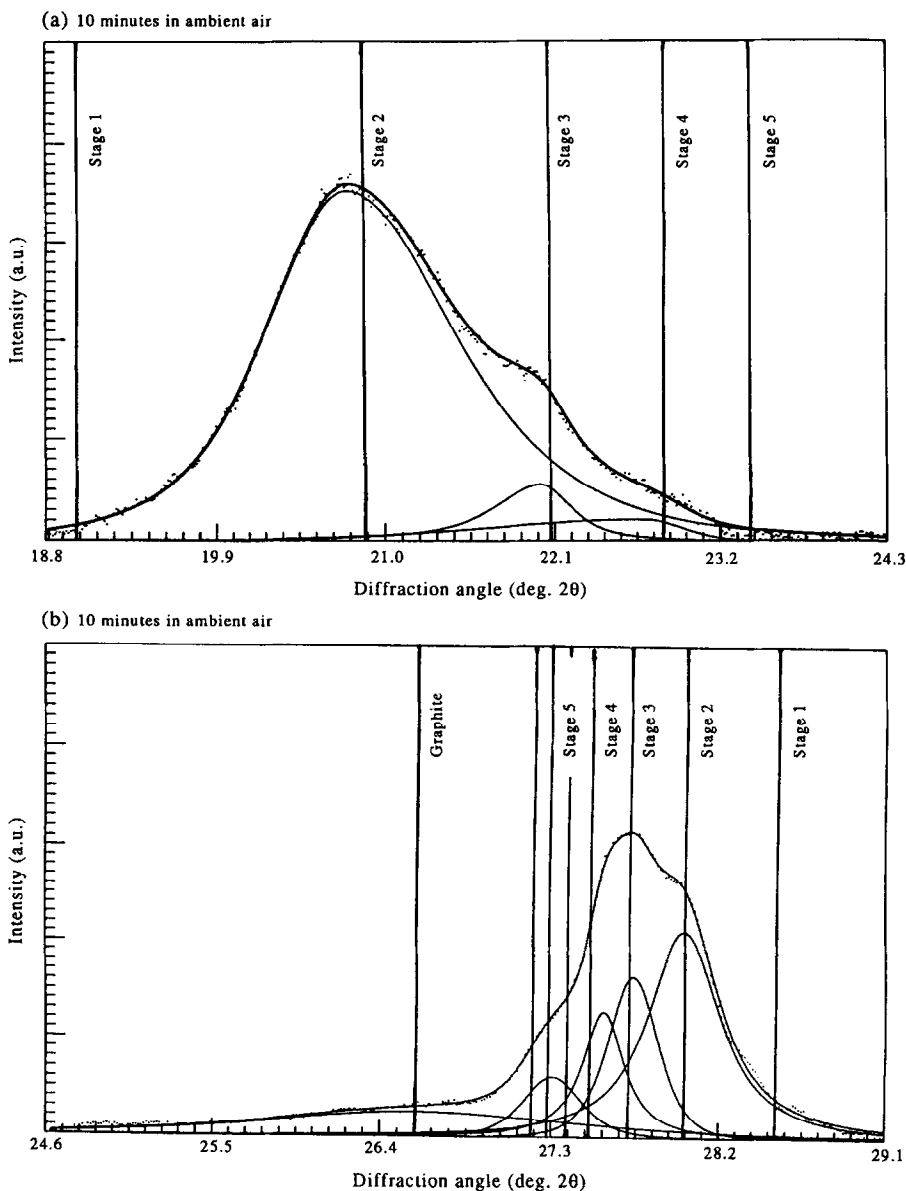


Fig. 1. The diffraction profile of  $\text{CuCl}_2$ -intercalated graphite, measured after 10 minutes in ambient air. The angle positions of the peaks for pure stages are marked by vertical lines. (a)  $2\text{-}\theta$  range  $18.8\text{--}24.3^\circ$ ; (b)  $2\text{-}\theta$  range  $24.6\text{--}29.1^\circ$ .

Following the evolution of the profiles of the diffraction lines and the line positions during deintercalation, one can see three main characteristics (see Figs 1–4):

- (a) The peak maxima are displaced from the positions of pure stages during the first 30 minutes in ambient air and at any time in boiling water. This indicates the presence of stacking disorder (see Hendricks and Teller[13], or Seul and Torney[14]).
- (b) The asymmetry of diffraction profiles observable especially in low angle  $2\text{-}\theta$  range at the beginning of deintercalation in ambient air and at any time in boiling water indicates a strong concentration

gradient accompanied of course by the presence of mixed stages.

- (c) The pure stages observable after 30 minutes in ambient air do not show any significant changes in their line profiles during the next 220 minutes. That means that the size of coherent domains in the direction perpendicular to the layers remains constant.

The comparison of the diffraction patterns in ambient air and in boiling water points to certain features, common for both cases:

- The diffraction profiles show the gradual transfer of intensity from lower to higher stages during the

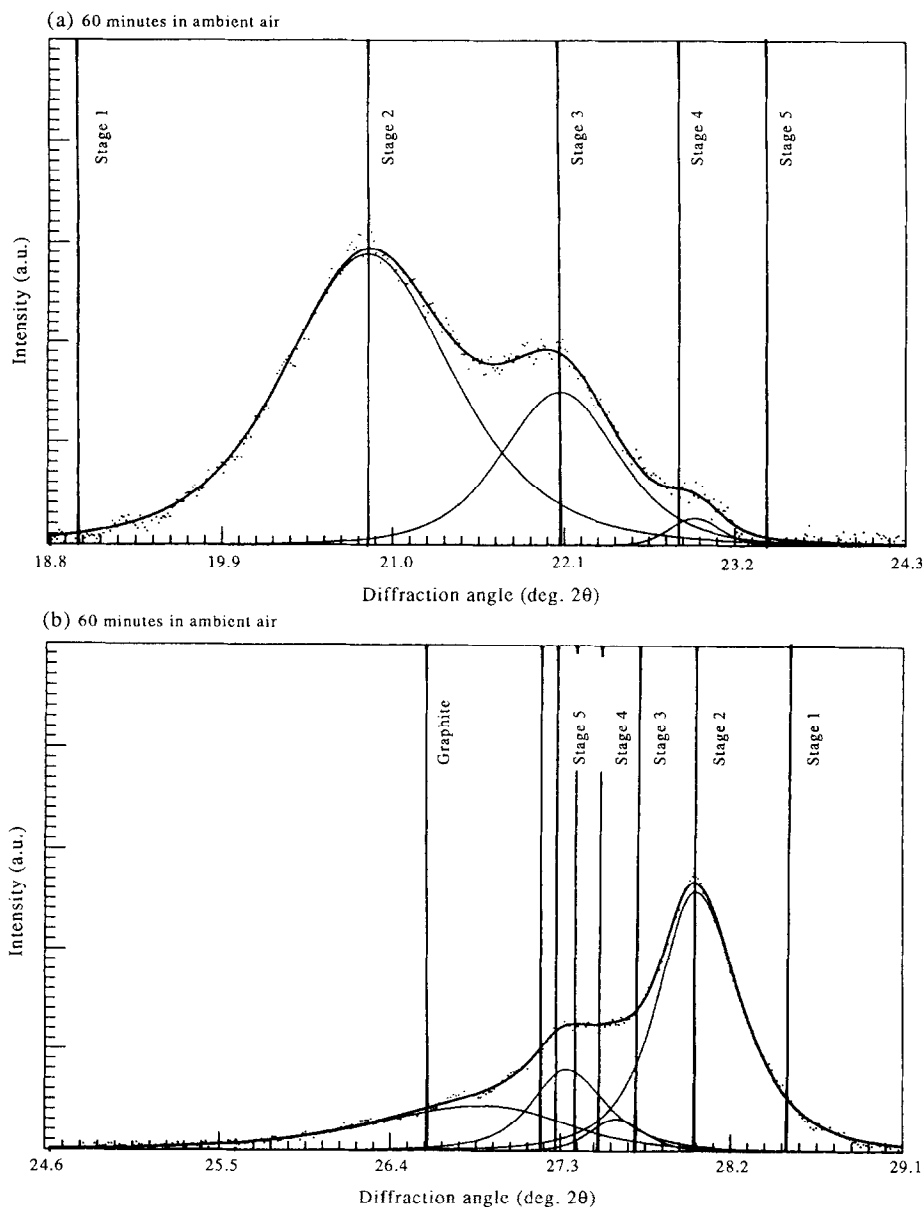


Fig. 2. The diffraction profile of  $\text{CuCl}_2$ -intercalated graphite, measured after 60 minutes in ambient air.

decomposition as a result of a gradual decrease of the  $\text{CuCl}_2$  content in the sample.

- The shift of maxima and changes of the profiles are continuous, which indicates the presence of stacking disorder and confirms diffusion as the ruling process.

The most pronounced difference between deintercalation in boiling water and in ambient air is, as expected, in kinetics. The shift of diffraction profiles to higher stages and the intensity redistribution are more striking in boiling water, indicative of a much faster decrease of  $\text{CuCl}_2$  content than in ambient air.

Another characteristic feature of deintercalation in boiling water is the presence of pure graphite at the edge of the powder platelets (see the graphite

peak in Figs 3 and 4). In the case of ambient air we can only observe a very broad peak near the graphite position, corresponding to the region of randomly stacked intercalant layers in graphite, with a very low concentration of  $\text{CuCl}_2$ .

In ambient air a strong tendency of the system to create pure stages has been observed (see Fig. 2). After 60 minutes, stage 2 occupies 45% and stage 3 18% of the sample volume. These pure stages remain preserved in the sample, with a slight decrease of their content, until the end of the measurements (250 minutes). In contrast to the observations in ambient air, the pure stages were not observable in the diffraction patterns after treatment in boiling water, even after 60 minutes.

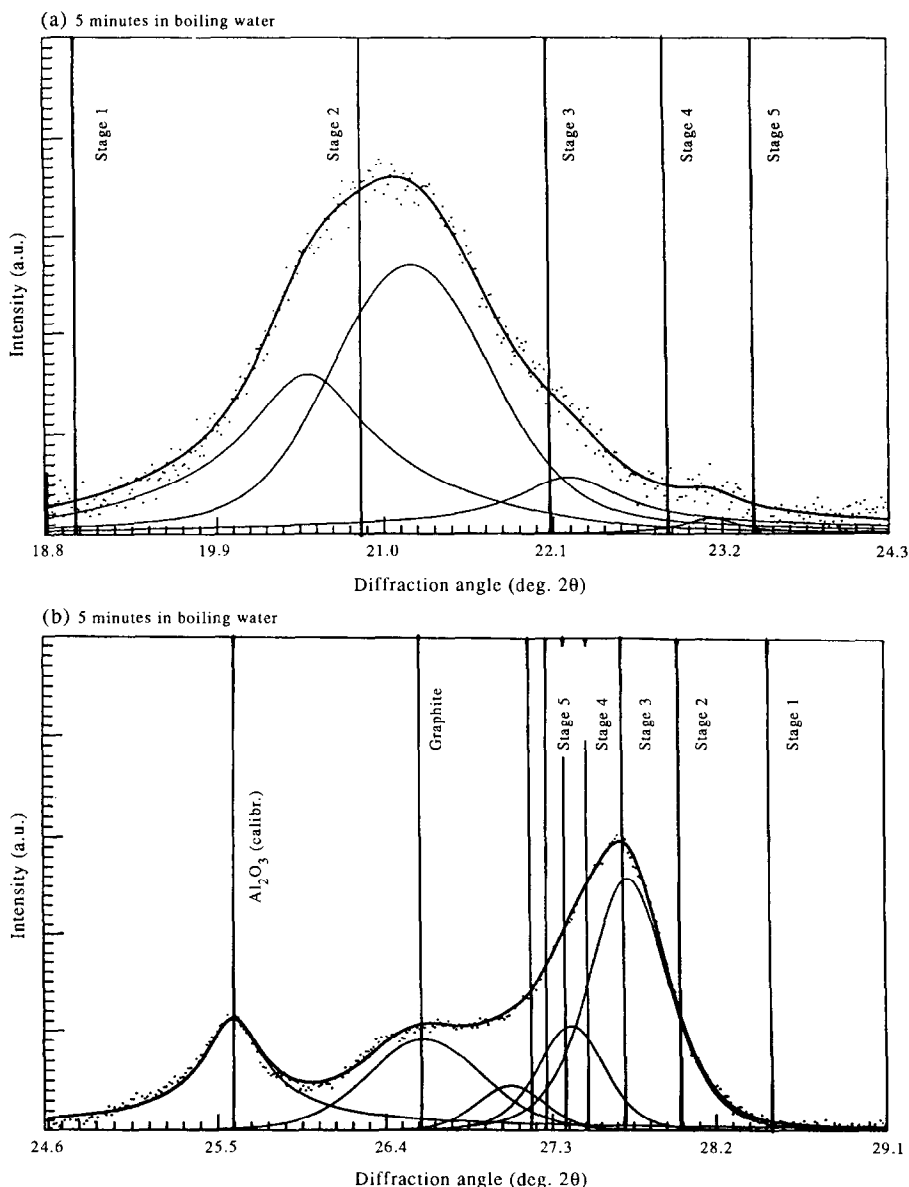


Fig. 3. The diffraction profile of  $\text{CuCl}_2$ -intercalated graphite, measured after 5 minutes in boiling water.

#### 4. CONCENTRATION PROFILES IN POWDER PARTICLES

An estimation of the concentration gradient is based on the quantitative phase analysis, i.e. on the volume content of the phases (pure or mixed stages), corresponding to the individual peaks in the fitted diffraction profiles. As the diffusion pathways of the intercalant in the host lattice, and consequently the flux of intercalant, are pointed along the radial direction of the disk-shaped particles, the concentration gradient can be illustrated by a schematic diagram, showing the course of  $\text{CuCl}_2$  concentration along the radius of average disk-shaped particles of intercalate. Optical microphotographs of partially intercalated powder particles [15] support this model for intercalant transport.

The concentration profiles in average powder particles, calculated on the basis of the present results are illustrated in Figs 5 and 6. The concentrations of mixed stages were derived from the angle positions of corresponding peaks. The lengths of the horizontal lines were calculated from the volume content of the individual phases (pure or mixed stages) corresponding to the fitted diffraction peaks (see Figs 1–4).

##### 4.1 Deintercalation in ambient air

The course of the concentration gradient after 10 minutes in ambient air (Fig. 5) shows a large region of mixed stage 1+2, two small regions of mixed stages 2+3, 3+4 and the region of high stages  $n > 5$ , where the  $\text{CuCl}_2$  concentration tends to zero at the edge of the particles. As the last peak, corresponding

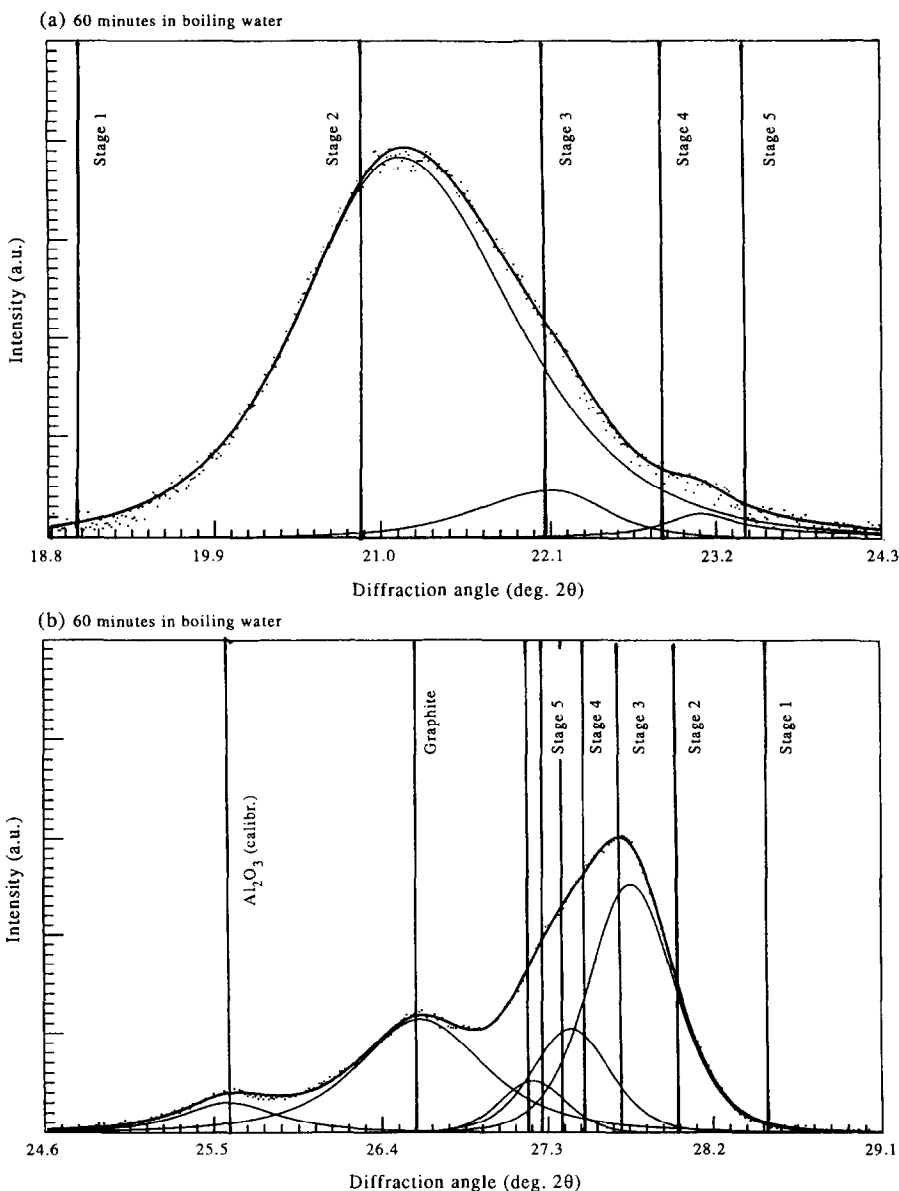


Fig. 4. The diffraction profile of  $\text{CuCl}_2$ -intercalated graphite, measured after 60 minutes in boiling water.

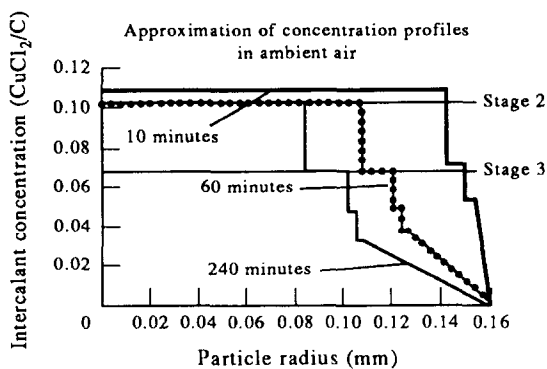


Fig. 5. Approximation of the concentration profiles in the radial direction of an average powder particle, after exposure to ambient air: for 10 minutes (heavy solid line), 60 minutes (dotted line) and 240 minutes (thin solid line).

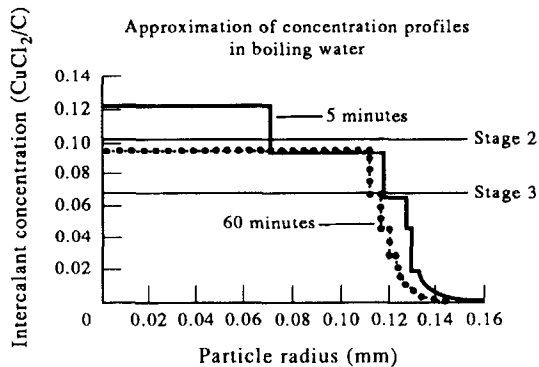


Fig. 6. Approximation of concentration profiles in the radial direction of an average powder particle, after exposure to boiling water: for 5 minutes (heavy solid line) and 60 minutes (dotted line).

to mixed high-index stages near graphite (Fig. 1, second part), is extremely broadened, indicating the wide range of concentrations, we used the linear dependence to approximate the concentration gradient at the edge of the particles exposed to ambient air. The concentration profile after 10 minutes in air just reflect the fact that at the beginning of the diffusion process the gradient of chemical potential is the main driving force for the redistribution of intercalant in the graphite structure. This is the period of highest diffusivity, when the mixed disordered stages are dominant in the sample.

The concentration profile at mixed stages is approximated by the horizontal lines, although, in fact, these regions are not completely homogeneous. The profile asymmetry of corresponding peaks (see Figs 1(a), 3(a) and 4(a) indicates the presence of transition zones with a steep concentration gradient at the border of each homogeneous region. However, the more detailed analysis of peak profiles is complicated in this case by the presence of microstress, distorting the graphite layers at the border of Daumas-Hérol domains [5] (see Fig. 7) and contributing to the diffraction line broadening.

With a decreasing amount of intercalant in the host structure and consequently decreasing gradient of chemical potential, the diffusivity decreases and the role of electrostatic and elastic interactions increases. These forces drive the system to the pure stage ordering. As a result, large regions arise in the sample, with a concentration lying in a very narrow range (usually described as line compounds). The distinct pure stages observable after 60 minutes in ambient air (Fig. 2) confirm this trend. The peak profiles corresponding to these pure stages are symmetric, without any pronounced evidence of stacking disorder for stages  $n < 4$ ; that means that the transition zones between the pure stages are very narrow at room temperature. This is completely in agreement with Kirczenow's calculations [1] of staging phase diagrams.

interface between pure stages 2 and 3

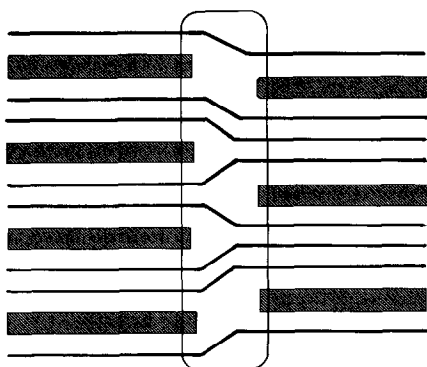


Fig. 7. The distortion of carbon layers in the transition zone between the pure stage 2 and 3.

#### 4.2 Deintercalation in boiling water

Comparing Figs 5 and 6, we can see a different character of concentration profiles in ambient air and boiling water. Due to the higher temperature and consequently higher diffusivity, we can see a dramatic decrease of intercalant content even after 5 minutes in boiling water, in comparison with 10 minutes in air. Higher diffusivity prefers the mixed disordered stages, whereas the stages tend to separate from one another at lower diffusivity. Moreover, relatively large regions at the edge of the particles are completely deintercalated in boiling water and consequently the gradient of chemical potential becomes more steep in the rest of every particle with increasing fractions of pure graphite. As a result, the diffusivity remains high, which also supports the occurrence of mixed stages.

The diagrams approximating the phase composition in an average disk-shaped powder particle after 60 minutes in boiling water and in ambient air are shown in Fig. 8 to illustrate the main characteristics of the deintercalation reaction in ambient air and in boiling water and to emphasize the following differences:

- the difference in kinetics (deintercalation in boiling water is much faster);

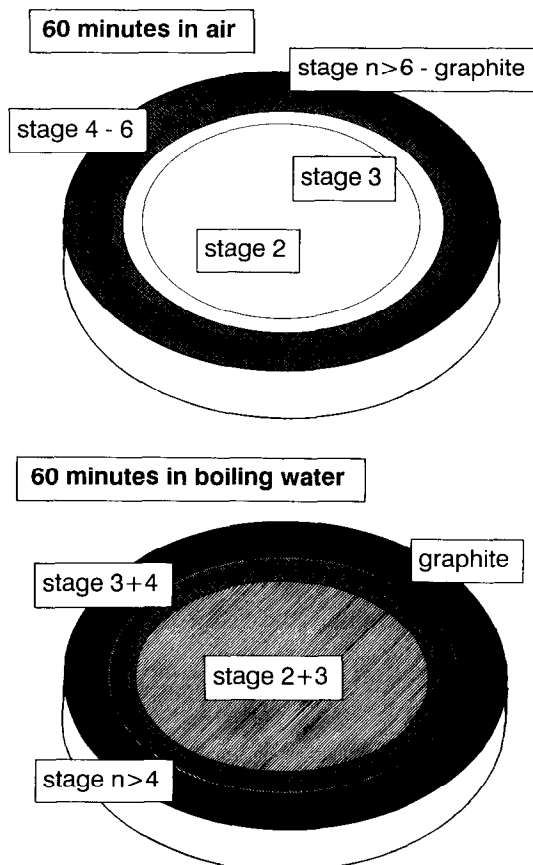


Fig. 8. Diagram showing the comparison of the phase composition in an average powder particle after 60 minutes in ambient air and boiling water.



- the difference in composition of the border regions at the edge of the flakes (i.e., pure graphite with the small islands of high stages in boiling water and mixed high stages in ambient air);
- large regions of pure stages 2 and 3 in air and prevailing mixed stages in boiling water.

The peak corresponding to pure graphite, observed in the diffraction pattern after exposure to boiling water, shows the presence of completely deintercalated regions in the sample. The additional EPMA/EDS analysis revealed the small islands of  $\text{CuCl}_2$  even near the edges of the flakes. It follows, in real samples treated in boiling water, that the region near the edge of the particle consists of pure graphite with small intercalant islands. An error function has been used for the approximation of the average concentration profile near the edges of the flakes, as usual in the case of one-dimensional diffusion process.

### 5. MECHANISM OF DEINTERCALATION

Following the theoretical studies, summarized in the introduction to the present paper, we can consider the mechanism of deintercalation as a result of competition between three main forces:

- the electrostatic interactions between intercalant layers, leading to the ordering of layers (staging);
- the long-range elastic interactions of two-dimensional islands of intercalant, driving a mixed-stage or randomly staged crystal to pure-stage ordering;
- a gradient of chemical potential, driving the transport of intercalant in the sample.

The present results show the influence of temperature on the joint effect of these forces.

The evolution of the diffraction patterns showed a continuous shift of the peak maxima during deintercalation. This indicates the continuous changes of concentration, confirms the dominant role of diffusion, and consequently supports the classification of the staging phase transition as continuous, in agreement with theory [1].

The effect of temperature on deintercalation manifests itself in two ways:

- Firstly, the difference is in kinetics, as is evident from the comparison of diffraction and concentration profiles for both cases.
- Secondly, a larger overlap of peaks, and no pure stages, as observed in the diffraction pattern for the reaction with boiling water in comparison with that for ambient air. This indicates the large transition zones between eventual small pure-stage regions and confirms the theoretical results, presented by Kirczenow [1]. The phase diagrams calculated by Kirczenow show an increasing overlap of phases with increasing temperature; that

means that the degree of disorder increases, the transitions broaden and the highest attainable pure stage decreases with increasing temperature. This trend is also observable in the present measurements.

### 6. CONCLUSION

Summarizing the present results, we can conclude that the real-time quantitative phase analysis enables the visualization of the phase composition at any time of diffusion-ruled deintercalation reaction, and reveals the movement of phase boundaries and the changes of the concentration gradient along the radial direction of disk-shaped particles. Consequently the present results contribute to a better understanding of staging transitions and confirm the theoretical predictions concerning the mechanism and character of these phase transitions. Moreover, the detailed study of the stability of GIC is important for numerous practical applications, suggested for these compounds (see e.g. [16] and [17]).

*Acknowledgements*—This publication is based on work supported by the Grant Agency of the Czech Republic, under grant no. 205/94/0468 and the Grant Agency of Charles University, Prague, under grant no. GAUK 33. We also thank the Fond der Chemischen Industrie (Germany) and the US-Czechoslovak Science and Technology Joint Fund and International Center for Diffraction Data for financial support.

### REFERENCES

1. G. Kirczenow, *Phys. Rev.* **B31**, 5376 (1985).
2. S. A. Safran, *Phys. Rev. Lett.* **B44**, 937 (1980).
3. S. H. Anderson Axdal and D. D. L. Chung, *Carbon* **25**, 377 (1987).
4. S. A. Safran and D. R. Hamann, *Phys. Rev. Lett.* **42**, 1410 (1979).
5. N. Daumas and A. Herold, *C.R. Acad. Sci. Paris* **C268**, 373 (1969).
6. A. Ansart, *Synth. Metals* **23**, 455 (1988).
7. K. F. van Malssen, R. Peschar and H. Schenk, *J. Appl. Cryst.* **27**, 302 (1994).
8. E. Stumpp, *Mater. Sci. Engng* **31**, 53 (1977).
9. R. Kužel, Jr, DIFPATAN (computer program), Faculty of Mathematics and Physics, Charles University, Prague (1991).
10. F. H. Chung, *J. Appl. Cryst.* **8** 17 (1975).
11. E. Vila and A. Ruiz-Amil, *Powder Diffract.* **3**, 7 (1988).
12. T. Doležal, Theses, Faculty of Mathematics and Physics, Charles University, Prague (1994).
13. S. Hendricks and E. Teller, *J. Chem. Phys.* **10**, 147 (1942).
14. M. Seul and D. C. Torney, *Acta Cryst.* **A45**, 381 (1989).
15. A. J. Jacobson, in *Solid State Chemistry Compounds* (Edited by A. K. Cheetham and P. Day). Clarendon Press, Oxford (1992).
16. S. A. Solin, in *Advances in Chemical Physics* (Edited by I. Prigogine and Stuart A. Rice). John Wiley & Sons, New York (1982).
17. G. R. Hennig, in *Progress in Inorganic Chemistry 1*, (Edited by F. A. Cotton), pp. 125-201, Wiley Interscience, New York (1959).